

Supporting Information

Photoconverting waste amphiphiles at the mild air-water interface into easily separable value-added products

Qin Dai^{a, b, c, d}, Xiaoyu Zhang^a, Jingyi Lin^a, Tao Cui^a, Wenbo Wang^{a, c}, Guangfei Yu^{a, d},
and Hongbin Cao^{a, b, c}, He Zhao^{a, b, c *}

^a Institute of Process Engineering, State Key Laboratory of Biochemical Engineering, Key Laboratory of Biopharmaceutical Preparation and Delivery, Chinese Academy of Sciences, Beijing 100190, China

^b Chemistry & Chemical Engineering Data Center, Chinese Academy of Sciences, Beijing 100190, China

^c University of Chinese Academy of Sciences, Beijing, 100049, China

^d MOE Key Laboratory of Resources and Environmental Systems Optimization, College of Environmental Science and Engineering, North China Electric Power University, Beijing 102206, China

Corresponding Author

*hzhao@ipe.ac.cn

Table of Contents

Fig. S1 Schematic diagram of converting 4 types of waste surfactants into value-added products and their collection and analysis.	3
Fig. S2 GC-MS spectra from different waste surfactants under interfacial photochemistry.....	4
Fig. S3 UV-vis spectra of different pure surfactants.	5
Fig. S4 ESR spectra of DMPO-OH obtained from (a) nonanol and (b) nonyl amine under interfacial photoirradiation.....	6
Fig. S5 The mechanism and pathway of the formation of nonanal from (a) nonanol and (b) nonyl amine under interfacial photoirradiation.....	7
Fig. S6 The peaks of gaseous products from different surfactants upon different photoirradiation time: (a) nonanol; (b) nonanal; (c) NA; (d) nonyl amine.....	8
Fig. S7 Nonanal, NA and nonyl amine solutions before (0 h) and after photoirradiation (6 h)	9
Fig. S8 (a) Comparison of total gas production (/mM) and (b) solid FNs-containing solutions obtained from mixed system and individual system after interfacial photoirradiation.	10
Fig. S9 Comparison of the Henry's constant of gaseous products with their precursors.	11
Fig. S10 Effect of humic acid on the (a) yield and (b) distribution and of gas products.....	12
Fig. S11 The conversion of nonanal to NA upon photoirradiation for 5h.....	13
Fig. S12 Changes of pH value of different surfactant system with respect to time.	14
Fig. S13 The morphological distribution of NA (a) and Nonyl amine (b) at different pH.	15
Fig. S14 Comparison of first vertical excited energies between neutral NA and NA anion, neutral nonyl amine and nonyl amine cation.	16
Fig. S15 Optimized ground state (S_0), singlet (S_1) and triplet (T_1) structures of various surfactants.	17
Table S1 Energies for reactants and products calculated at M062X/def2TZVP level.....	18
Table S2 Calculated reaction energies at M062X/def2TZVP level.....	19
Table S3 Cost estimation for the process of converting 1 ton of NA wastewater into high value-added products	20
Notes and references	21

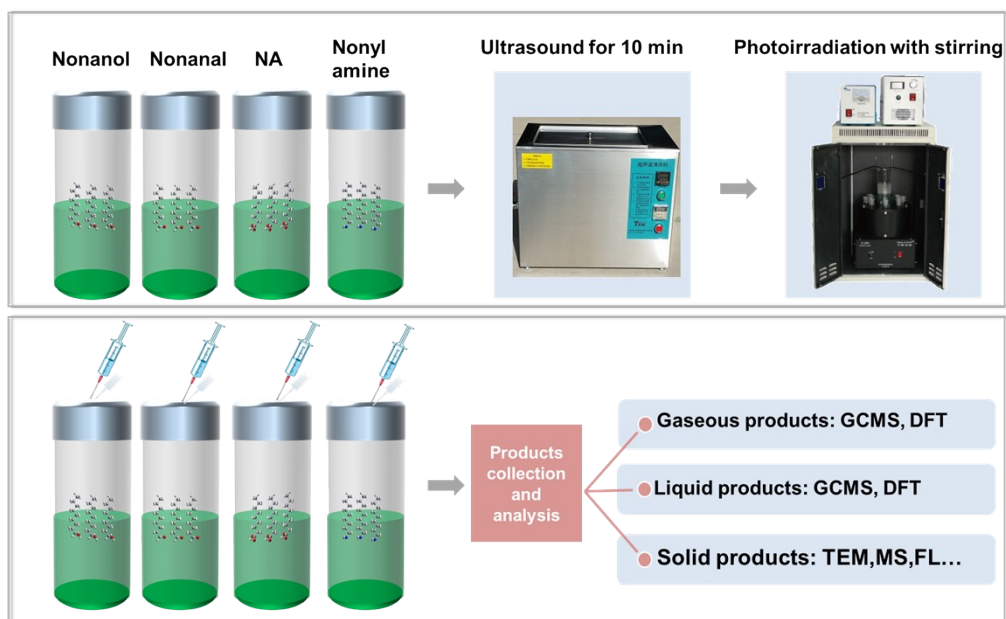


Fig. S1 Schematic diagram of converting 4 types of waste surfactants into value-added products and their collection and analysis.

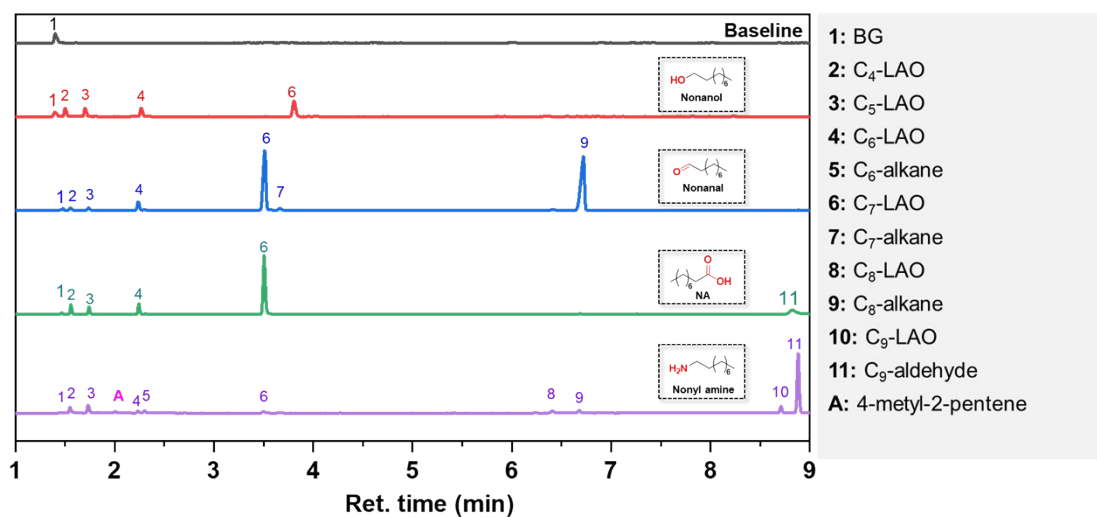


Fig. S2 GC-MS spectra from different waste surfactants under interfacial photochemistry.

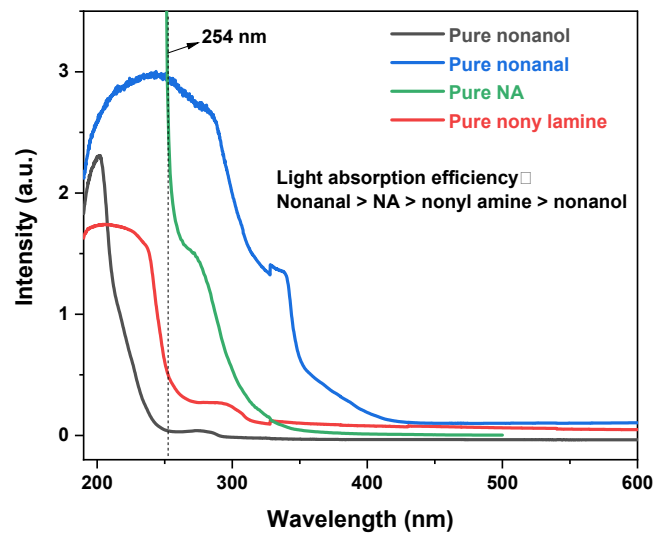


Fig. S3 UV-vis spectra of different pure surfactants.

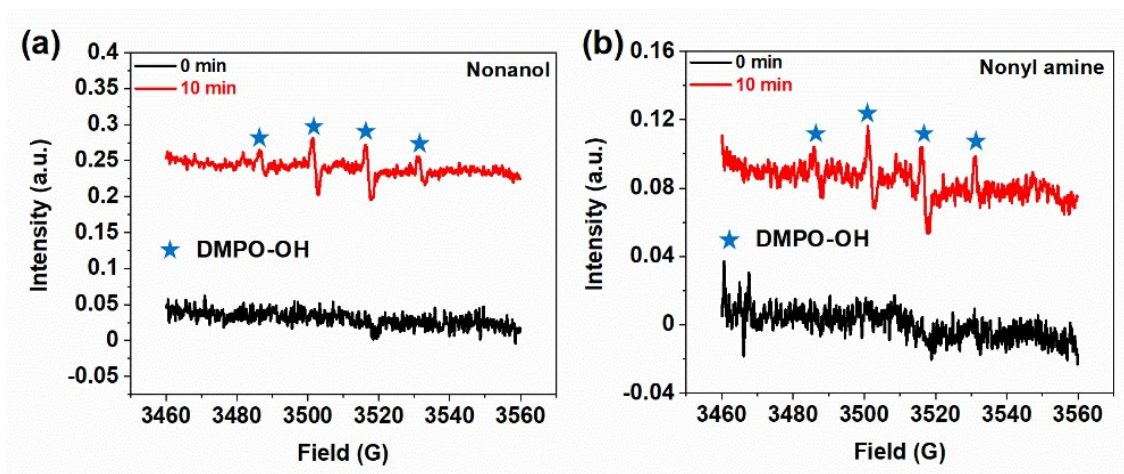


Fig. S4 ESR spectra of DMPO-OH obtained from (a) nonanol and (b) nonyl amine under interfacial photoirradiation.

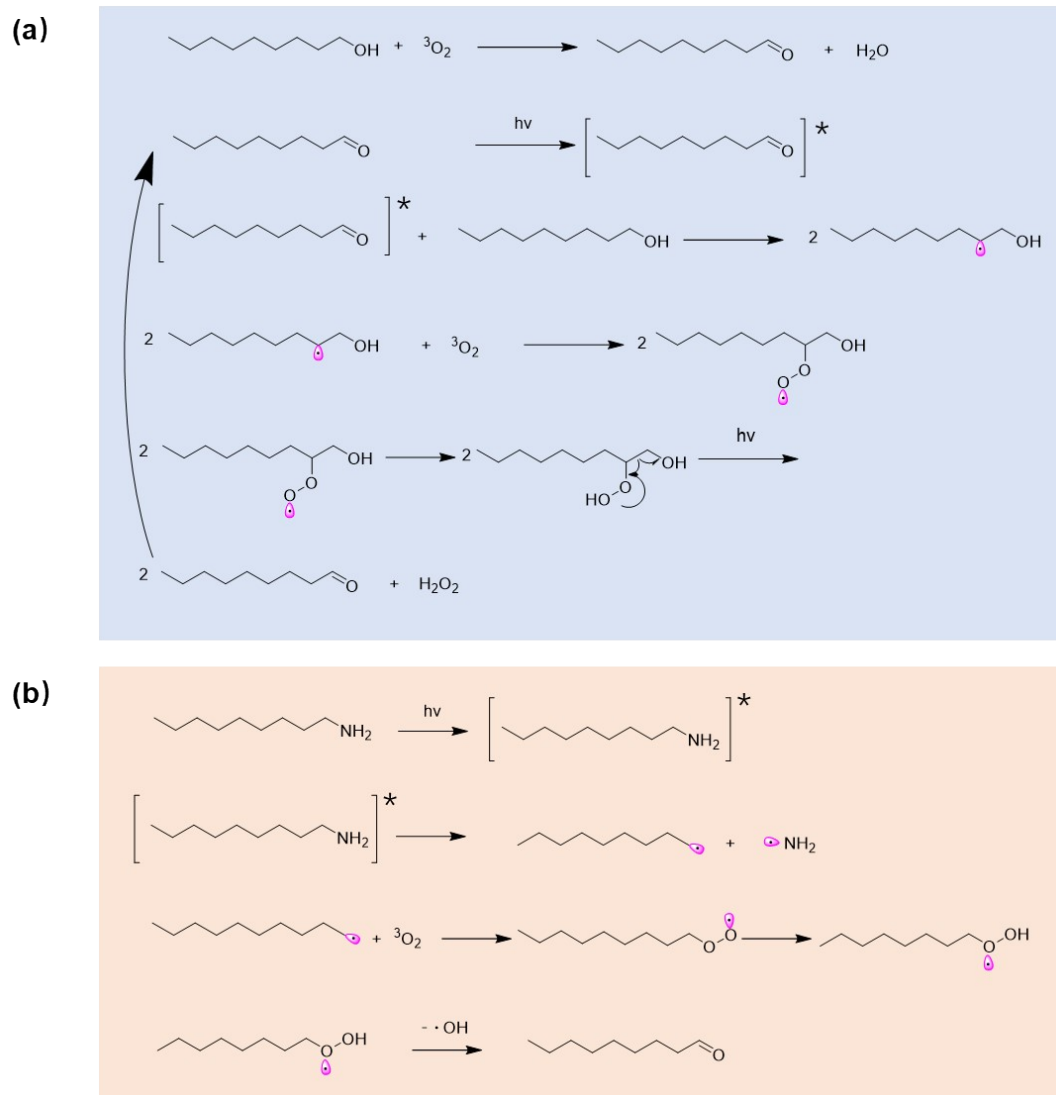


Fig. S5 The mechanism and pathway of the formation of nonanal from (a) nonanol and (b) nonyl amine under interfacial photoirradiation.

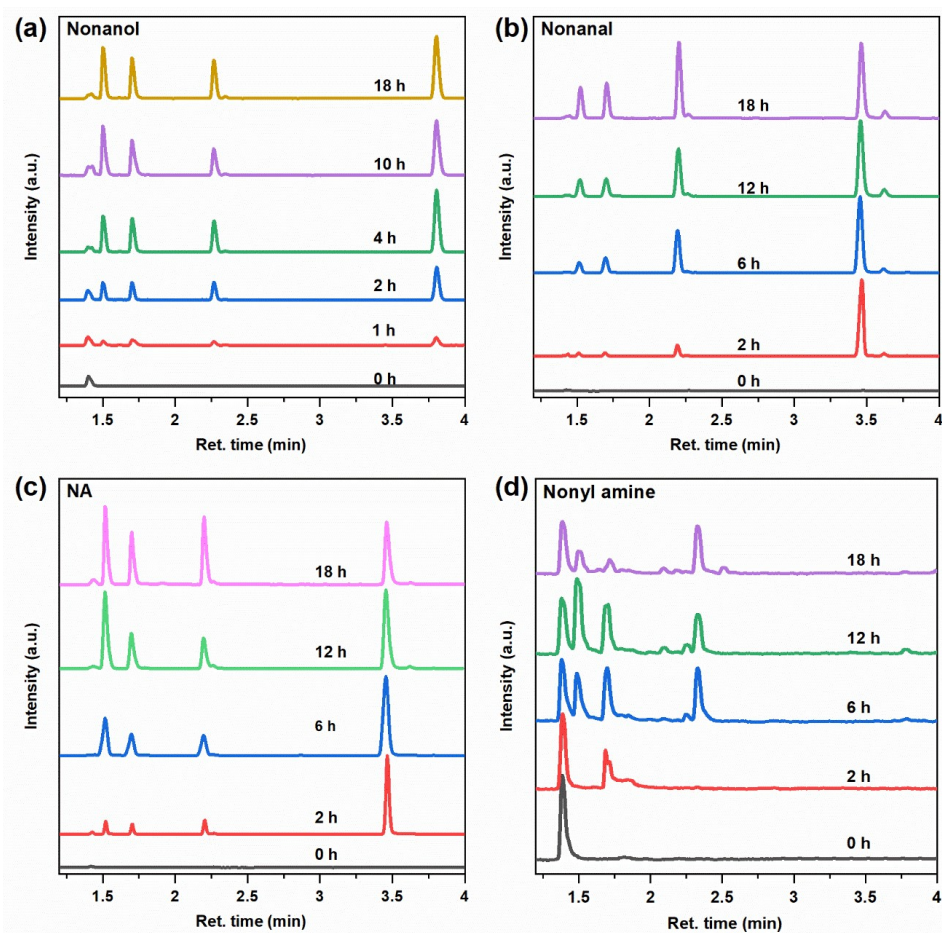


Fig. S6 The peaks of gaseous products from different surfactants upon different photoirradiation time: (a) nonanol; (b) nonanal; (c) NA; (d) nonyl amine.

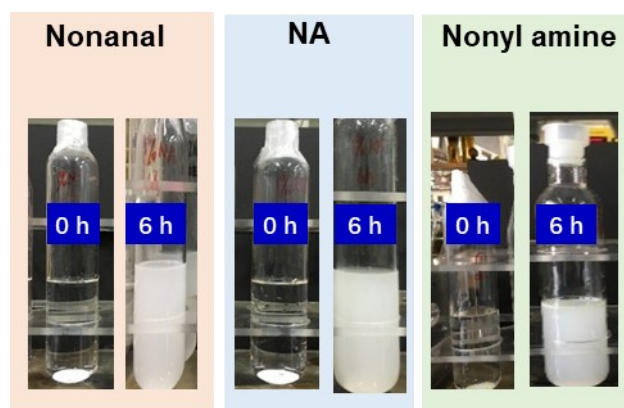


Fig. S7 Nonanal, NA and nonyl amine solutions before (0 h) and after photoirradiation (6 h)

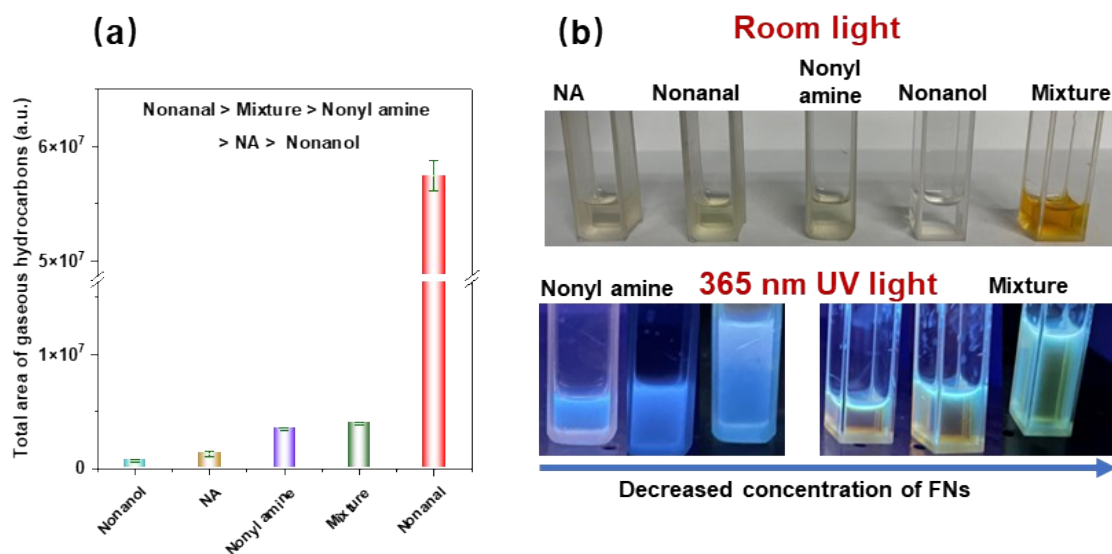


Fig. S8 (a) Comparison of total gas production (/mM) and (b) solid FNs-containing solutions obtained from mixed system and individual system after interfacial photoirradiation.

Surprisingly, **Fig.S8b** that the conversion tendency of solid fluorescent nanoparticles (FNs) in the mixed system is strengthened. This is because the darker yellow color of mixed system under room light compared to the individual system indicating its high concentration of FNs. Under 365-nm UV light, the FNs-containing solution from mixed system displayed a significant fluorescence quenching effect, while the FNs-containing from nonyl amine alone did not, further supporting the production of higher concentrations of FNs in the mixed system.¹ The above results indicate that mixing different types of surfactants together can synergistically significantly enhance their conversion to solid-phase FNs. The mechanism of synergistic enhancement for FNs production in the mixed system would be investigated in the future.

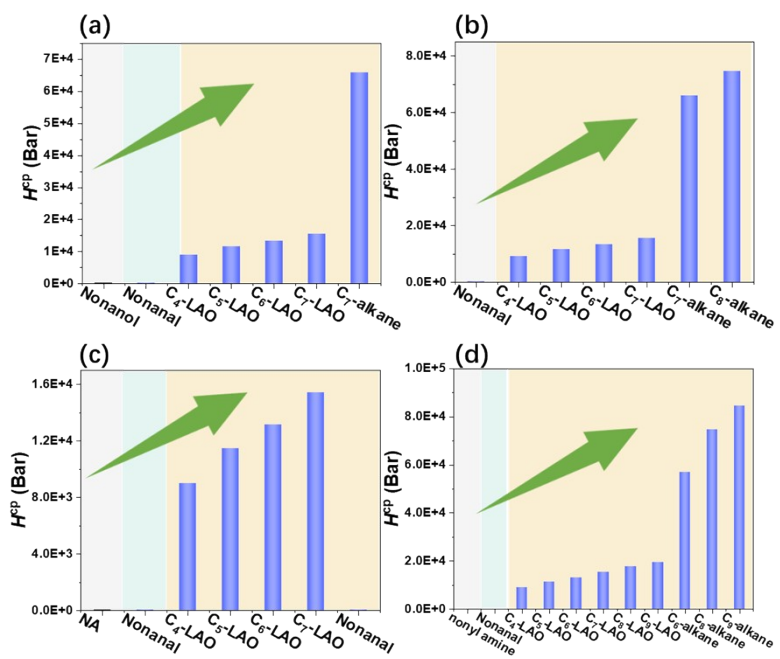


Fig. S9 Comparison of the Henry's constant of gaseous products with their precursors.

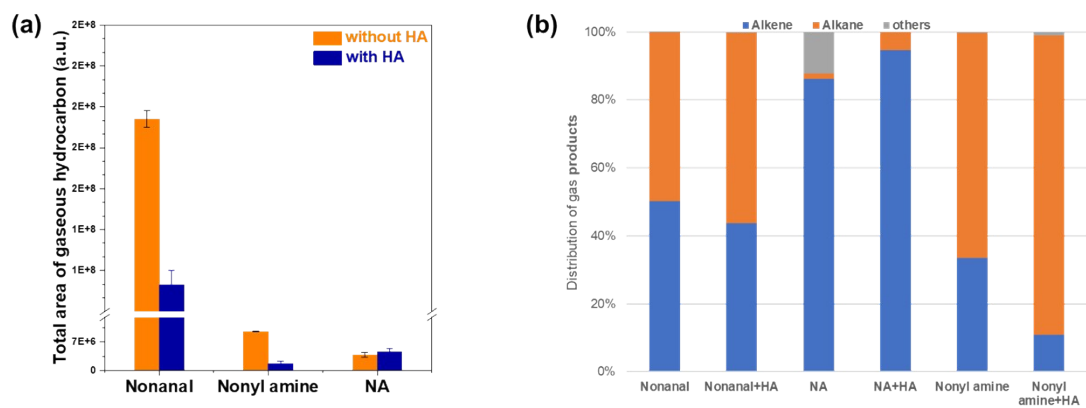


Fig. S10 Effect of humic acid on the (a) yield and (b) distribution and of gas products.

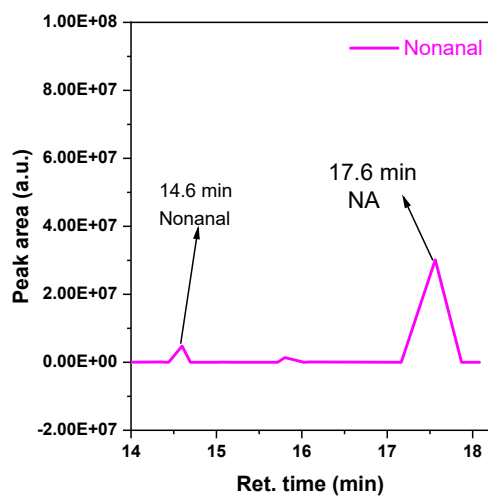


Fig. S11 The conversion of nonanal to NA upon photoirradiation for 5h.

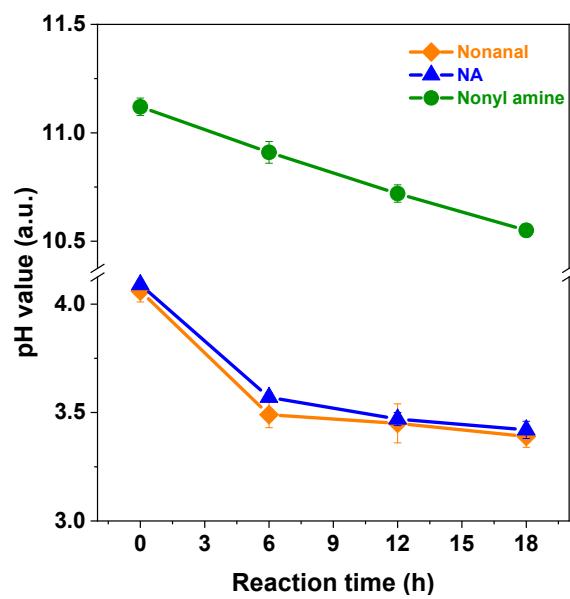


Fig. S12 Changes of pH value of different surfactant system with respect to time.

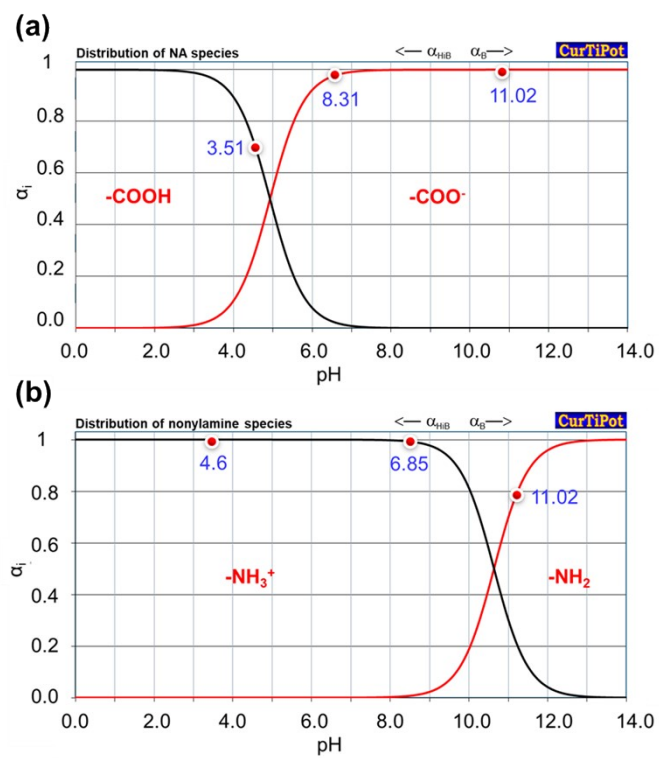


Fig. S13 The morphological distribution of NA (a) and Nonyl amine (b) at different pH.

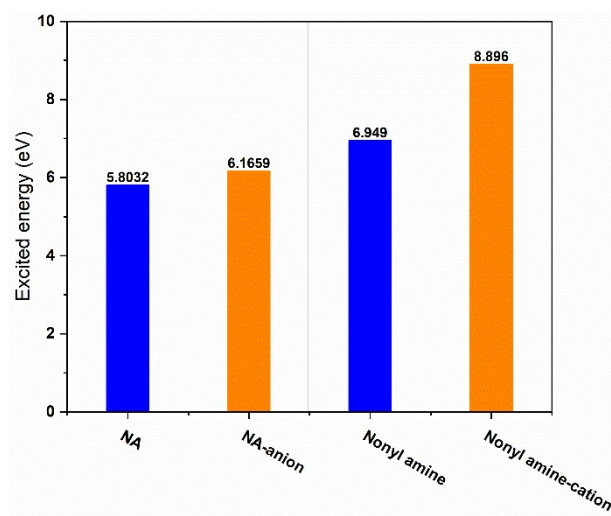


Fig. S14 Comparison of first vertical excited energies between neutral NA and NA anion, neutral nonyl amine and nonyl amine cation.

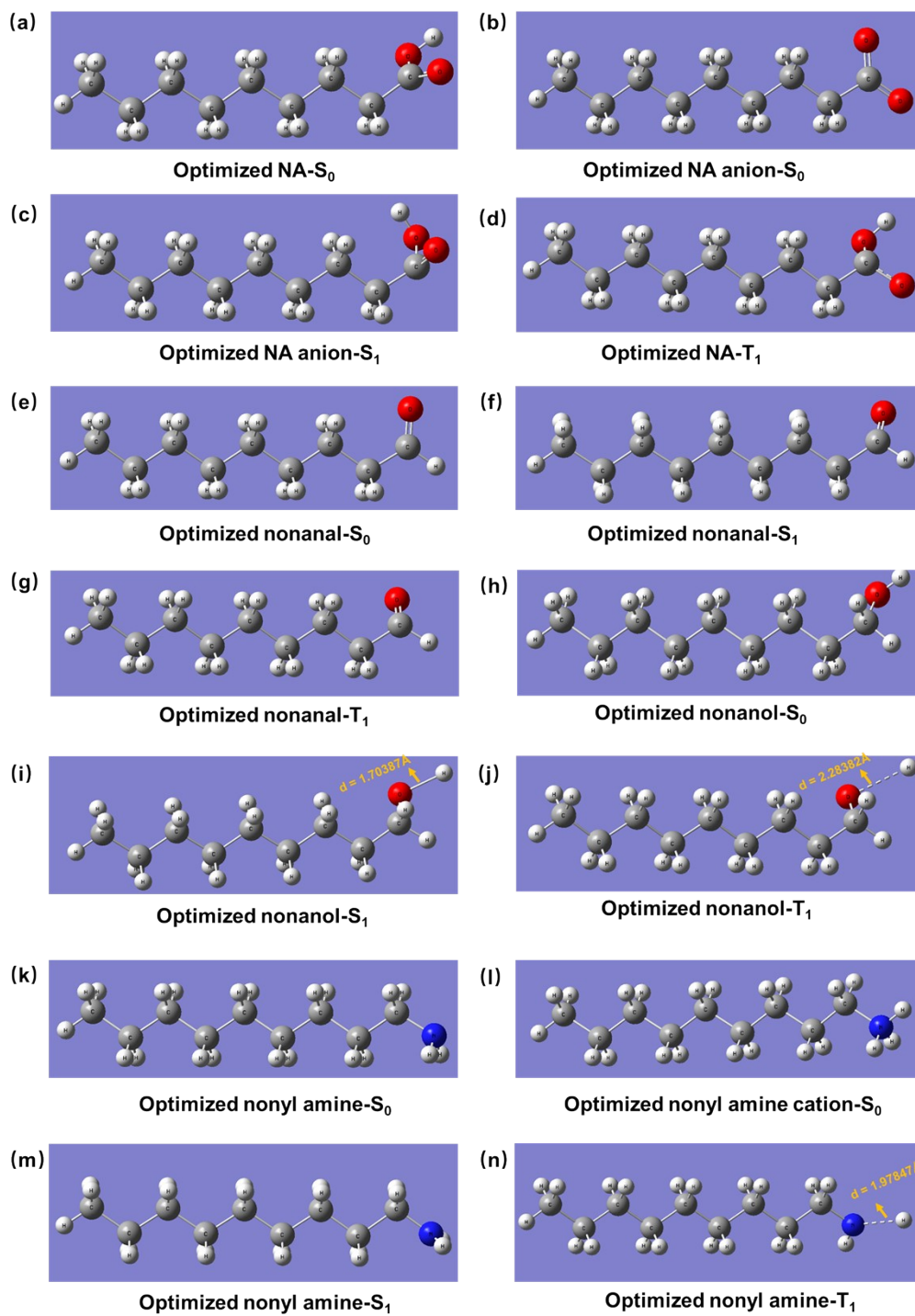


Fig. S15 Optimized ground state (S₀), singlet (S₁) and triplet (T₁) structures of various surfactants.

Table S1 Energies for reactants and products calculated at M062X/def2TZVP level.

Name	Zero-point energy (hartree)	Thermal correction to Enthalpy (hartree)	Thermal correction to Gibbs free energy (hartree)	Single point energy (hartree)	H (298.15K, hartree)	G (298.15K, hartree)
Nonanol (S ₀)	0.280638	0.295045	0.239513	-430.182754	-429.887709	-429.943241
Nonanol (S ₁)	0.269277	0.284155	0.227332	-429.963023	-429.887709	-429.735691
Nonanol (T ₁)	0.266077	0.280196	0.225591	-430.00267	-429.887709	-429.777079
CH ₃ (CH ₂) ₇ -COH	0.266953	0.281384	0.225162	-429.524335	-429.242951	-429.299173
CH ₃ (CH ₂) ₇ -C(OO)OH	0.277044	0.293248	0.231639	-579.918691	-579.625443	-579.687052
CH ₃ (CH ₂) ₇ -C(OOH)OH	0.289036	0.305706	0.24392	-580.56324	-580.257534	-580.31932
Nonanal (S ₀)	0.256452	0.270324	0.215694	-428.977769	-428.707445	-428.762075
Nonanal (S ₁)	0.253182	0.267389	0.212106	-428.835733	-428.568344	-428.623627
Nonanal (T ₁)	0.25303	0.267217	0.210734	-428.85002	-428.582803	-428.639286
NA (S ₀)	0.262612	0.277378	0.218827	-504.245779	-503.968401	-504.026952
NA (S ₁)	0.258403	0.273829	0.215125	-504.060099	-503.78627	-503.844974
NA (T ₁)	0.258782	0.274113	0.214761	-504.0826	-503.808487	-503.867839
NA anion (S ₀)	0.249106	0.263617	0.206018	-503.776594	-503.512977	-503.570576
Nonyl amine (S ₀)	0.293253	0.307892	0.251743	-410.307906	-410.000014	-410.056163
Nonyl amine (S ₁)	0.282658	0.297638	0.241057	-410.084388	-409.78675	-409.843331
Nonyl amine (T ₁)	0.279758	0.293952	0.239215	-410.133702	-409.83975	-409.894487
Nonyl amine cation (S ₀)	0.309069	0.323717	0.267645	-410.760895	-410.437178	-410.49325
CH ₃ (CH ₂) ₆ -CH ₂ •CH ₂	0.2601	0.274048	0.218958	-354.28542	-354.011372	-354.066462
•NH ₂	0.019203	0.022984	0.000244	-55.874531	-55.851547	-55.874287
CH ₃ (CH ₂) ₆ •CH•CH ₂	0.245981	0.25983	0.204966	-353.620117	-353.360287	-353.415151
CH ₃ (CH ₂) ₆ •CH ₂	0.231571	0.244143	0.192813	-314.978184	-314.734041	-314.785371
•CH ₂ NH ₂	0.050184	0.054584	0.02702	-95.191524	-95.13694	-95.164504
³ O ₂	0.004023	0.007329	-0.015914	-150.32731	-150.319981	-150.343224
¹ O ₂	0.004011	0.007317	-0.014886	-150.268976	-150.261659	-150.283862
H ₂ O	0.021392	0.025172	0.003748	-76.433708	-76.408536	-76.42996
H ₂ O ₂	0.027054	0.031192	0.005469	-151.559208	-151.528016	-151.553739
H•	0	0.00236	-0.010654	-0.498162	-0.495802	-0.508816

Table S2 Calculated reaction energies at M062X/def2TZVP level.

Chemical reaction	ΔG (kJ/mol) or cleavage energy
$2\text{CH}_3(\text{CH}_2)_8\text{OH} + {}^3\text{O}_2 = 2{}^3\text{CH}_3(\text{CH}_2)_7\text{-C(H)=O} + 2\text{H}_2\text{O}$	-561.137613
${}^3\text{CH}_3(\text{CH}_2)_7\text{-C(H)=O} + \text{CH}_3(\text{CH}_2)_7\text{-COH} = 2\text{CH}_3(\text{CH}_2)_7\text{-}\bullet\text{COH}$	-41.5327845
$2\text{CH}_3(\text{CH}_2)_7\text{-}\bullet\text{COH} + \text{O}_2 = 2\text{CH}_3(\text{CH}_2)_7\text{-C(OO}\bullet\text{)OH}$	-117.2417025
$2\text{CH}_3(\text{CH}_2)_7\text{-C(OOH)OH} = \text{H}_2\text{O}_2 + \text{CH}_3(\text{CH}_2)_7\text{-C(H)=O}$	9.205003
$\text{CH}_3(\text{CH}_2)_8\text{-NH}_2 = \bullet\text{NH}_2 + \text{CH}_3(\text{CH}_2)_7\text{-CH}_2\bullet$	303.0195
$\text{CH}_3(\text{CH}_2)_8\text{-NH}_2 = \bullet\text{CH}_2\text{NH}_2 + \text{CH}_3(\text{CH}_2)_6\text{-CH}_2\bullet$	279.059144
$\text{CH}_3(\text{CH}_2)_7\text{-CH}_2\bullet = \bullet\text{H} + \text{CH}_3(\text{CH}_2)_6\text{-}\bullet\text{CH-CH}_2\bullet$	374.0523595

Table S3 Cost estimation for the process of converting 1 ton of NA wastewater into high value-added products

Methods	NA concentration in water (mM)	Product parameter (C ₇ -LAO)	Key reagent and unit price	Reagent cost (\$/m ³)	Energy cost (\$/m ³)	Operating cost (\$/m ³)	Ref.
Chemical heterogeneous catalysis	0.05-2 ²⁻⁴	Selectivity: 45-80% Conversion rate: 0.7-11.1%	Catalyst: Pt/C (40-45 \$/g) Norit activated carbon (450 \$/ton) N ₂ (4.7-4.8 \$/m ³)	115.7-214.3	1028.5-1285.7	1144.3-1500	5
Chemical homogeneous catalysis	0.05-2 ²⁻⁴	Selectivity: 84-91% Conversion rate: 59-78%	Catalyst: Pt (40-45 \$/g) γ-valerolactone (3805-3880) \$/ton	1628.6-1691.4	30-40	1658.6-1731.5	6
Enzymatic catalysis	0.05-2 ²⁻⁴	Product yield: 40-70%	NADPH: 21500 \$/mol	>9890		>9890	7, 8
Gas-water interfacial photoirradiation	0.05-2 ²⁻⁴	Selectivity: 87%-91% Conversion rate: 60-99%			800-511.14	800-511.14	Our work

Note: energy cost was calculated based on the electricity (0.1085\$/kWh)⁹ and reagent cost was calculated based on the market price and literatures.

Notes and references

1. D. Zhou, D. Li, P. Jing, Y. Zhai, D. Shen, S. Qu and A. L. Rogach, *Chem. Mater.*, 2017, **29**, 1779-1787.
 2. Grassian, *Chem Sci*, 2020, **11**, 10647-10656.
 3. S. Rossignol, L. Tinel, A. Bianco, M. Passananti, M. Brigante, D. J. Donaldson and C. George, *Science*, 2016, **353**, 699-702.
 4. D. Hua M. Luo, N. A. Wauer, K. J. Angle, A. C. Dommer, M. Song, C. M. Nowak, R. E. Amaro and V. H, *Environ. Sci. Technol.*, 2020, **54**, 13448-13457..
ng, J. Wang, H. Xia, Y. Zhang, F. Bao, M. Li, C. Chen and J. Zhao, *Environ. Sci. Technol.*, 2020, **54**, 13448-13457.
 5. J. A. Lopez-Ruiz and R. J. Davis, *Green Chem.*, 2014, **16**, 683-694.
 6. S. H. Hopen Eliasson, A. Chatterjee, G. Occhipinti and V. R. Jensen, *ACS Sustain. Chem. Eng.*, 2019, **7**, 4903-4911.
 7. X. Wang, T. Saba, H. H. P. Yiu, R. F. Howe, J. A. Anderson and J. Shi, *Chem*, 2017, **2**, 621-654.
 8. C. Lu, F. Shen, S. Wang, Y. Wang, J. Liu, W.-J. Bai and X. Wang, *ACS Catal.*, 2018, **8**, 5794-5798.
 9. W. Gao, Z. Sun, H. Cao, H. Ding, Y. Zeng, P. Ning, G. Xu and Y. Zhang, *Journal of Cleaner Production*, 2020, **256**, 120217.
- Huang D, Wang J, Xia H, et al. Enhanced photochemical volatile organic compounds release from fatty acids by surface-enriched Fe (III)[J].